*Original research article*

# Evaluating the Effectiveness of Bond Strength Relative to Plain Reinforcement Bar Diameter in HVFA-SCC Beam Lap Splices

Ashar Natsir Sasmito[*], Stefanus Adi Kristiawan, Halwan Alfisa Saifullah

*Teknik Sipil, Universitas Sebelas Maret, Surakarta 57126, Indonesia*

**ABSTRACT**

The primary issue with Portland cement production, a critical component in concrete, is its considerable $CO_2$ emissions. An effective strategy to reduce $CO_2$ emissions from cement manufacturing involves using fly ash as a substantial replacement for cement. Experimental research has concentrated on comparing the bond strength of plain steel reinforcement with concrete constructed using High Volume Fly Ash - Self Compacting Concrete (HVFA-SCC). This comparison involves substituting at least 50% of the cement with fly ash. The experimental program includes six splice beam test specimens as controls. Additionally, this study compares the results with those from a control specimen bond database. The findings indicate that HVFA-SCC beams exhibit superior mean bond strength compared to other types of concrete.

**Keywords:** Bond strength; High Volume Fly Ash; Self-Compacting Concrete (SCC); Plain reinforcement; Splice Length

## 1. Introduction

The construction industry faces the dual challenge of advancing infrastructure development while utilizing sustainable materials. This research focuses on the use of High Volume Fly Ash (HVFA) in Self-Compacting Concrete (SCC) to enhance structural performance. Specifically, this study investigates the bond strength between plain steel reinforcement and HVFA-SCC beams. The objective is to provide a deeper understanding of how HVFA-SCC

can be utilized to maintain or improve structural integrity, contributing to more efficient and durable construction practices [1].

The integration of these advancements, specifically High Volume Fly Ash Self-Compacting Concrete (HVFA-SCC), has substantial potential to enhance sustainability in construction while maintaining or even improving structural performance standards [2]. However, the introduction of this material raises essential questions about the interaction between HVFA-SCC and traditional structural elements, particularly plain reinforcement bars that have long been used in construction.

The incorporation of High Volume Fly Ash (HVFA) in Self-Compacting Concrete (SCC) has been shown to improve strength, durability, and environmental sustainability. The addition of fly ash enhances compressive strength and durability while also reducing crack width and drying shrinkage [3]. Furthermore, there is also evidence that fly ash has a beneficial effect on strength development and resilience to external sulphate attacks [4]. Numerous studies have reviewed the potential for cost-effective production and the use of alternative materials in SCC [5, 6]. The synergistic effects of fly ash and other materials, such as silica fume, in enhancing the performance of HVFA-SCC have also been investigated [7].

According to a study by Zulu, increasing the percentage of fly ash up to 50% in SCC mixes can substantially reduce carbon emissions without compromising mechanical strength [8]. Replacing 25% of cement with fly ash has been reported to reduce carbon emissions by up to 17% [9]. Additionally, it has been demonstrated that SCC can be developed with an increased sand-to-aggregate ratio and up to 25% cement replacement with fly ash without re-

ducing strength [10]. Further research has explored the use of high-volume fly ash in SCC, finding that replacements up to 70% can be achieved without significant loss of strength [7, 11]. Studies have identified that fly ash can serve as a partial replacement for cement in SCC, with 30% being recognized as the most suitable mix [12, 13].

Prior to implementing HVFA-SCC reinforced concrete, it is crucial to comprehend its structural behaviour. The force distribution between the reinforcement and the surrounding concrete is a crucial aspect in determining the structural performance of concrete. The force distribution may be determined based on the bond strength and the development length. Bond strength significantly influences various aspects, such as the growth of tensile strength, the occurrence of transverse cracks, flexural curvature, the strength of anchorage at the ends, splice length, and the rotating capability of plastic hinges [14].

In general, the bond strength between reinforcement and concrete encompasses adhesion resistance, frictional resistance at the interface, and mechanical interlock of the reinforcement surface (ribs) with the concrete [15]. The chemical bond between the reinforcement and concrete is established through chemical processes that take place during the curing phase. This bond is the main factor that determines the strength of the bond, especially in the case of plain reinforcement. The initiation of interface cracks between the reinforcement and concrete leads to a drastic reduction in bond strength [16–18]. Factors such as concrete cover thickness, concrete properties, reinforcement diameter, surface characteristics of the reinforcement related to corrosion, the addition of stirrups, and casting position (effect on the top bars) all contribute to influencing bond strength [19–21].

Regarding the bond strength issues of reinforced concrete, several researchers have reported that the use of fly ash (FA) as a partial replacement for cement in specific compositions results in higher bond strength compared to conventional concrete and reduces the likelihood of reinforcement pullout from the surrounding concrete [14]. Studies have also indicated that SCC exhibits superior bond strength characteristics compared to conventional concrete. Research by Mohamed [22] demonstrated that the bond strength values in SCC are higher than those in ordinary concrete.

There are four most effective test methods for determining the bond strength between reinforcement and concrete: pull-out test, modified cantilever beam test, beam anchorage test, and splice test. Among these, splice testing is considered the most effective for determining development length, as it provides a more realistic stress state around the reinforcement [23]. The development of bond strength between steel reinforcement and concrete is directly related to splice length [24]. The magnitude of bond strength determines the required length of embedded reinforcement (splice length) so that the tensile stress in the reinforcement can effectively reach its yield stress [25].

One of the drawbacks of using splice length is the material wastage caused by the lapping of two reinforcement bars. Typically, the splice length used for most structural components is around 40 times the diameter of the reinforcement. Therefore, the larger the diameter, the longer the reinforcement, leading to increased wastage in lapping. Harinkhede et al. [26] noted that significant diameter steel reinforcement requires 15% more reinforcement for lap splicing. Kastiza [27] explained that the lap splice length for plain reinforcement

should be twice that of deformed (ribbed) reinforcement, with the same diameter and yield strength in conventional concrete.

In this context, High Volume Fly Ash Self-Compacting Concrete (HVFA-SCC) represents the latest advancement in concrete technology, combining the benefits of HVFA and SCC to meet high construction standards with minimal environmental impact. Despite extensive research on the mechanical properties and durability of HVFA-SCC, there remains significant scope to explore its performance in reinforced concrete applications, particularly regarding the interaction between concrete and plain reinforcement bars.

Research on the bond strength of HVFA-SCC concrete is limited, especially concerning the use of plain reinforcement. The issue with plain reinforcement (i.e., bars without lugs) is that, while not included in new designs, it is still prevalent in existing structures. Plain reinforcement was used in the United States and Canada until the mid-1950s, in Europe until the 1960s [28], and continues to be used in Indonesia. Slip failures often occur at reinforcement splice regions, particularly in beams reinforced with plain bars [29]. Plain reinforcement behaves differently from deformed bars due to the lack of mechanical interlock with the surrounding concrete.

The use of plain reinforcement, though not the primary choice in modern designs due to its lower bond strength compared to deformed bars, remains highly relevant. Many structures built in earlier eras still stand today, utilizing plain reinforcement as a core component. In some regions and countries, plain bars continue to be used due to factors like cost and availability. Therefore, understanding the interaction between plain reinforcement and innovative concrete such as HVFA-SCC is

crucial for assessing, designing, and renovating existing structures, as well as for new applications where plain reinforcement is still considered.

This research is essential because it is necessary to deeply understand the bond strength between plain reinforcement bars and HVFA-SCC. Adequate bond strength is essential for structural integrity, influencing load transfer, crack formation, and the deformation capacity of structural elements. Investigating the bond strength effectiveness in HVFA-SCC beams with plain reinforcement bar diameters at lap splices will not only fill existing knowledge gaps but also provide crucial guidelines for safer, more economical, and sustainable design and construction practices.

Thus, this research is worthy of investigation as it presents an opportunity to significantly advance our understanding of how high-performance and sustainable construction materials can be optimally utilized in the context of reinforced concrete, particularly with plain reinforcement that is still widely used. The results of this study contribute to enhancing structural performance, particularly in reinforcing plain steel bars in HVFA-SCC, and offer insights that may aid in reducing the environmental impact of new construction and retrofitting existing structures.

## 2. Research Methodology

This study utilizes an experimental methodology to assess the bonding strength between plain reinforcement and HVFA-SCC, with a specific focus on the impact of reinforcement diameter on the effectiveness of lap splice connections. The research methodology is designed to provide a thorough understanding of the interaction between plain reinforcement and HVFA-SCC and to develop applicable design and construction recommendations for practical implementation.

Test specimens are specifically designed to simulate real-life lap splice situations. HVFA-SCC will be produced with a specific proportion of fly ash replacing cement, aiming to meet the criteria for self-compacting properties and the desired mechanical performance. The primary variable being studied is the diameter of the plain reinforcement, which will be altered in many sizes to evaluate its impact on bond strength. The flowchart in Fig. 1 summarizes the sequential steps of our research.
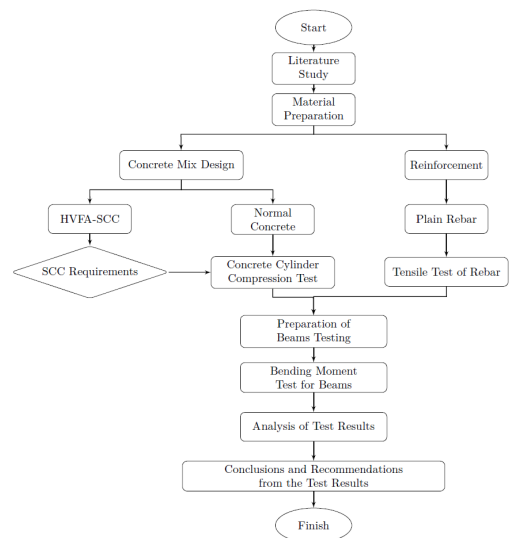


**Fig. 1.** Research methodology flowchart.

The research begins with a thorough Literature Review to gain a deep understanding of the issue being investigated and identify any gaps in existing research. This literature assessment contributes to the establishment of the theoretical and methodological structure of the research. After conducting a thorough review of the existing literature, the research progresses to the phase of Material Preparation. Currently, all the necessary materials for the experi-

ment, such as reinforcement and concrete, have been prepared.

The process of concrete preparation entails creating Concrete Mix Designs for HVFA-SCC, which stands for High Volume Fly Ash-Self-Compacting Concrete. The mix designs undergo testing to verify their compliance with the approved Self-Consolidating Concrete (SCC) standards. After material preparation, a Tensile Test of Reinforcement is conducted to determine the mechanical characteristics of the reinforcement used. This procedure is crucial to ensure that the reinforcement has sufficient strength for structural applications in this research.

Subsequently, a Concrete Cylinder Compression Test is conducted to assess the compressive properties of both varieties of concrete. This testing yields crucial data concerning the robustness and longevity of the concrete intended for construction purposes. Following that, beam testing preparation is conducted to prepare for the subsequent test, which is the beam splice length-bending moment test. The purpose of this test is to analyze the response of beams to bending moments, with a specific focus on evaluating the bond strength in splice beams.

The outcomes of all these tests are analyzed and examined during the Testing Results Analysis phase. This analysis involves evaluating the data gathered from multiple tests in order to generate scientifically based conclusions. Finally, the research concludes with an outline of Conclusions and Recommendations based on the test specimen results. This section highlights the main findings from the research and provides recommendations based on the test results and the potential for further research.

The data collected from the testing will be analyzed to determine the relationship between the diameter of the reinforcement and the bond strength in HVFA-SCC. This analysis will include using statistical methods to evaluate the significance of the reinforcement diameter's impact on bond strength and identify any trends or patterns that may emerge from the data.

There are effective test methods to determine bond strength between reinforcement and concrete, and one of them is splice testing. Splice testing is considered more effective for assessing bond strength because, according to Rabbat and colleagues, it represents "a more realistic stress-state around the reinforcement" [30].

The following section details the splice beam specimens used in this research to evaluate the effectiveness of bond strength between plain steel reinforcement and concrete.

## 2.1 Mixture design and properties

This section describes the process undertaken to develop the concrete mixture design using a high volume of cement substitutes. The HVFA-SCC mix was developed by optimizing binder and aggregate composition. It is proportioned by adjusting Portland cement and fly ash.

The concrete design aimed for this study is high-volume fly ash - Self-compacting concrete (HVFA-SCC) with a minimum compressive strength of 30 MPa while also meeting the requirements of SCC. The reinforcements reviewed include plain bars with diameters of 12 mm, 16 mm, and 19 mm. The mix design of HVFA-SCC follows the guidelines from EFNARC [31].

The amount of fly ash used is 50% of the total cement requirement. To achieve flowability in the test specimens, superplasticizer Consol P929-AS is added. The selection and procedures used are in accor-

dance with applicable standards, and the detail of material mix design calculations follows SNI-7656-2012 [32] and SNI-03-6468-2000 [33]. The details of the HVFA-SCC mix design for one m$^3$ are as follows: Fine aggregate 635 kg, Coarse aggregate 876 kg, Cement 275 kg, Fly ash 275 kg, Water 176 litres, and Superplasticizer 5.5 litres.

The fresh properties of the HVFA-SCC mixes, including slump flow, T50 slump flow, V-funnel time, and L-box ratio, were evaluated to ensure the mix met the required self-compacting concrete standards. These values are presented in Table 1, confirming the mix's compliance with ASTM specifications for workability and flowability.

Compressive strength testing of concrete was conducted following ASTM C39, which uses concrete cylinder test specimens with a height of 30 cm and a diameter of 15 cm. Testing was performed using a Universal Testing Machine (UTM) with a capacity of 1000 kN at the Materials Laboratory of the Faculty of Engineering, Universitas Sebelas Maret Surakarta. This study focuses on the use of concrete that has reached the age of 28 days and has a compressive strength of 33.12 MPa, shown in Table 5.

The fly ash (FA) used in this study comes from the Tanjung Jati B Power Station in Jepara, Central Java. The chemical composition of the fly ash, as tested according to ASTM C618-22, is provided in Table 2. This fly ash meets the specifications for Class F fly ash, which is suitable for use in High Volume Fly Ash Self-Compacting Concrete (HVFA-SCC).

## 2.2 Specimen splice beam

One method to test the overall bond integrity of a structure is through the splice test. The splice beam test involves using reinforcement bars connected within a beam

**Table 1.** Fresh properties of HVFA-SCC mixes.

| Property | Specification | Mix | Criteria |
|---|---|---|---|
| Slump flow (mm) | ASTM C1611 | 670 | 600 – 740 |
| T50 slump flow (s) | | 4.6 | <6.0 |
| V funnel (s) | ASTM C1621 | 9.1 | 6 – 12 |
| L box (%) | | 0.86 | 0.6 – 1 |

and then subjecting it to loads at four different points, as shown in Fig. 2. The test beam specimen has dimensions of 2000 mm × 150 mm × 250 mm. The longitudinal reinforcement used is plain bars.

The splice length is calculated using the development length formula provided in ACI 318-14 based on the beam test specimen's specifications. For the specimens to ensure bond failure occurs before the reinforcement yielding, 75% of the splice length ($l_s$) required by the code is selected for the test specimen. This value is chosen first based on prior research [34,35] and second to develop stresses in the steel that are below the yielding point to ensure failure in the splitting or slipping mode in all beam specimens. The yielding failure mode provides little or no information about the bond strength of reinforcement bars, and the aim is to compare the relative bond behavior of splice connections and not the ductility of the connection [36].

The top part of the longitudinal reinforcement uses plain bars with a diameter of ⌀8 mm, while the bottom part uses varying diameters of ⌀12 mm, ⌀16 mm, and ⌀19 mm. The tensile strength of the plain reinforcement bars was tested, and the results are shown in Table 3. These values confirm the suitability of the reinforcement for structural applications in this study.

The splice length is $0.75\,l_s$, and no stirrups are used at the splice. Along the area without splice length, stirrups are placed at a 70 mm interval. The splice lengths were calculated based on reinforce-

ment diameter and yield strength, as shown in Table 4. These values were critical for determining the bond strength performance in HVFA-SCC beams.

The concrete cover distance $c$ from the base of the reinforcement to the concrete surface is 25 mm. The test setup for the beam with splice length is shown in Fig. 2.

The diameter of the reinforcement and the splice length are variables investigated for their impact on bond strength. The data observed in this test are the load $P$, the deflection of the beam, and the strain on the tension reinforcement in the splice region. Beam deflection is measured with two LVDTs, while strain is detected by a strain gauges (SG) mounted on the tension reinforcement.

The required length $l_s$ in the splice beam testing can be calculated based on the critical bond strength $\tau_{cr}$ of HVFA-SCC concrete [36]. The use of this value aims to anticipate potential variations in the quality of beam test specimen production if there are lower-quality outcomes.

**Table 2.** Chemical compositions of fly ash.

| Elements | Content Amount (%) |
|---|---|
| $SiO_2$ | 43.82 |
| $Al_2O_3$ | 15.58 |
| FeO | 12.13 |
| CaO | 14.34 |
| MgO | 6.30 |
| $Na_2O$ | 2.99 |
| $K_2O$ | 1.30 |
| $TiO_2$ | 0.71 |
| $SO_3$ | 1.62 |
| LOI | 0.34 |

**Table 3.** Results of the Tensile Test for Plain Reinforcement.

| $D$ (mm) | Def (mm) | $f_y$ (MPa) | $f_u$ (MPa) |
|---|---|---|---|
| 8 | 7.70 | 340 | 470 |
| 12 | 11.72 | 347 | 485 |
| 16 | 15.71 | 340 | 476 |
| 19 | 18.7 | 350 | 490 |

**Table 4.** Calculated Requirements for Splice Length ($l_s$).

| $D$ (mm) | $f_y$ (MPa) | $\tau_{cr}$ (MPa) | $l_s$ (mm) | $0.75l_s$ (mm) |
|---|---|---|---|---|
| 12 | 405 | 3.05 | 398.7 | 299.0 |
| 16 | 415 | 3.05 | 544.8 | 408.6 |
| 19 | 392 | 3.05 | 611.0 | 458.3 |

**Note:** $D$ is the diameter and $f_y$ is the yield strength of the reinforcement.

**Table 5** Compressive Strength Test Results for Concrete Specimens at Different Ages.

| Sample | Age (Days) | $\rho$ (kg/m$^3$) | $P_{max}$ (kN) | $f_c'$ (MPa) | $\overline{f_c'}$ (MPa) |
|---|---|---|---|---|---|
| 1 | | 2323 | 340 | 19.25 | |
| 2 | 7 | 2291 | 310 | 17.55 | 18.40 |
| 3 | | 2293 | 325 | 18.40 | |
| 4 | | 2321 | 460 | 26.04 | |
| 5 | 14 | 2327 | 440 | 24.91 | 25.76 |
| 6 | | 2302 | 465 | 26.33 | |
| 7 | | 2304 | 565 | 31.99 | |
| 8 | 21 | 2331 | 540 | 30.57 | 30.67 |
| 9 | | 2318 | 520 | 29.44 | |
| 10 | | 2319 | 590 | 33.40 | |
| 11 | 28 | 2329 | 570 | 32.27 | 33.12 |
| 12 | | 2308 | 595 | 33.69 | |

**Note:** W is the weight, $\rho$ is the density, $P_{max}$ is the maximum load, and $f_c'$ is the compressive strength of the concrete.

### 2.3 Bond strength HVFA-SCC

In this study, the focus is placed on testing the bond characteristics between reinforcement and HVFA-SCC concrete through a series of splice-beam tests. Specimens consisting of three types of beams, which included a control beam, were created to evaluate the bond performance of HVFA-SCC. During testing, three parameters were recorded for each test specimen.
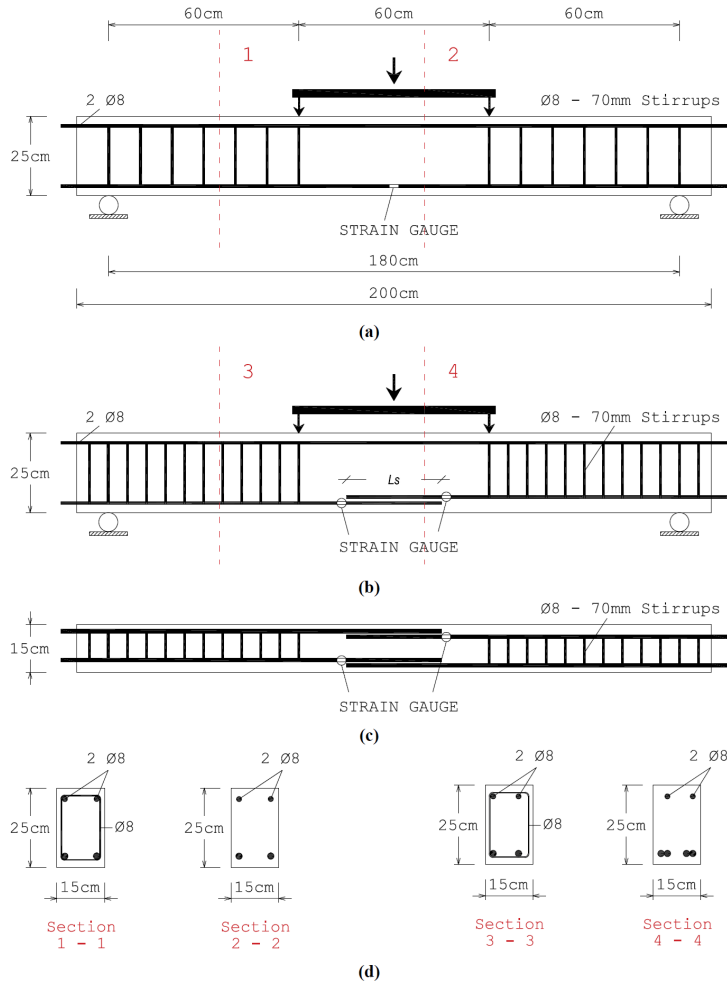
**Fig. 2.** Beam details without transverse stirrups in the loading area (a) control beam, (b) splice beam, (c) bottom view of the splice beam, and (d) cross section.

These values include the applied load, the corresponding mid-span deflection ($\Delta$), and the corresponding strain at the end of each reinforcement splice.

Table 6 summarizes the compressive strength at the time of testing ($f_c'$), the cracking load ($P_{cr}$), the ultimate load ($P_{ult}$), and the steel stress ($f_s$). The steel stress recorded at the time of specimen failure is determined by averaging three strain readings from each strain gauge on a structural component and then multiplying by the elastic modulus of the steel determined

from the tensile test of the reinforcement.

The average bond strength ($\tau$) is calculated using Equation 2.1 from the stress computed on the reinforcement bars at the time of failure as follows:

$$\tau = \frac{A_s \times f_s}{\pi \times D \times l_s} = \frac{D \times f_s}{4 \times l_s}, \qquad (2.1)$$

where $A_s$ represents the cross-sectional area of the reinforcing bar, $D$ is the diameter of the reinforcement, and $l_s$ signifies the splice length of the reinforcement in concrete. The value of $\tau$ indicates the bond strength be-

tween the concrete and the reinforcement, which is crucial for structural stability.

To enable direct comparison of test results with varying compressive strengths, the average bond strength ($\tau_{\text{test}}$) from each test is normalized using Equation 2.2:

$$\tau_{\text{normalized}} = \frac{\tau_{\text{test}}}{\sqrt{f_c}}. \qquad (2.2)$$

The design compressive strength ($f_c$) for the HVFA-SCC mix is 33 MPa. The strength during testing for each mix design is reported in Table 5. The one-quarter strength used in Equation 2.2 is based on the development equation in ACI 408R-03. Both the original average bond strength and the normalized bond strengths are presented in Fig. 8.

# 3. Test Results and Discussions
## 3.1 Crack patterns in splice beams

Observing the crack patterns that form can help understand the behaviour of beams under applied loads. These crack patterns provide valuable information about the type of failure the beam experienced, whether it was flexural or shear failure. The behaviour of the beam under applied loads is significantly reflected through the formed crack patterns. Analyzing these crack patterns allows for determining whether the beam undergoes flexural failure or shear failure.

Flexural crack patterns typically form longitudinally along the beam and occur in the areas of maximum moment. This crack indicates the deformation of the beam under bending loads, the top of the beam experiences compression, while the bottom is subjected to tension during bending. Evenly spaced and well-distributed cracks indicate that the beam is effectively designed and functioning to withstand

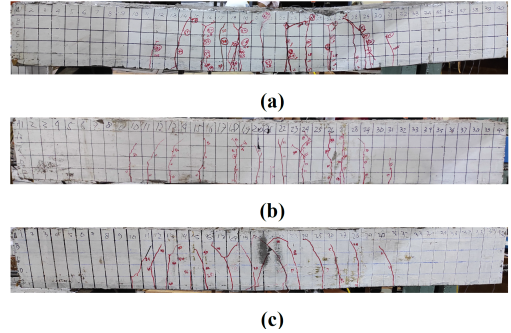bending loads, suggesting appropriate stress distribution.



**Fig. 3.** Crack patterns of HVFA-SCC control beam test specimens: (a) K-12-NS, 12 mm rebar; (b) K-16-NS, 16 mm rebar; (c) K-19-NS, 19 mm rebar.

Conversely, characteristic shear crack patterns are inclined or diagonal, often observed near supports or in areas with high shear forces. These cracks indicate that the beam may struggle to withstand shear forces, which, without adequate reinforcement, could lead to shear failure. Shear cracks highlight the importance of reinforcement against shear forces, such as the use of stirrups, to enhance the beam's performance under shear loads.

Through the analysis of these crack patterns, we can identify design needs or improvements to enhance the beam's resistance to various failure modes. These observations are vital in developing an understanding of beams' structural performance and guiding them towards more effective and safer structural design improvements.

Fig. 3 shows the crack pattern on the control beam. The applied load caused cracks to form in the beam. The cracks that appeared are flexural cracks with a vertical orientation. The location of the first flexural crack was observed in the middle of the span (in the area of constant moment). In the region of maximum moment, the beam experienced significant tensile stress due to

the applied load. This tensile stress initiated the formation of flexural cracks, which first appeared between the two load points and supports. As the applied load increased, these initial flexural cracks propagated, and additional vertical cracks formed, extending towards the compression zone. The progression of these cracks reflects the gradual redistribution of internal forces within the beam, ultimately leading to localized failure as the concrete in the compression zone reached its capacity. The control beam was more ductile and did not undergo sudden collapse. The test results concluded that the failure that occurred was flexural. The absence of shear cracks in the specimen indicates that shear failure did not occur.
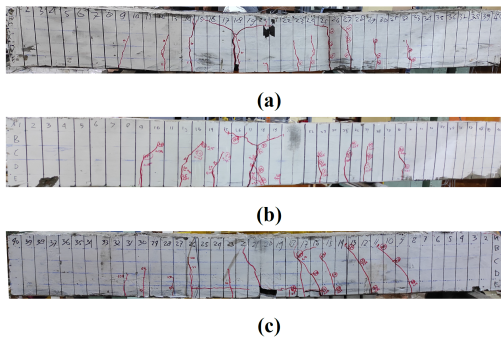


**Fig. 4.** Crack patterns of HVFA-SCC splice beams with specified splice lengths: (a) 0.75-12-NS, 12 mm rebar; (b) 0.75-16-NS, 16 mm rebar; (c) 0.75-19-NS, 19 mm rebar, all with $0.75l_s$.

Fig. 4 shows all the beams failed in bond, experiencing either slippage failure or splitting. In almost all splice beams, the first flexural crack occurred around the end of the splice length in the area of constant moment. As the load increased, additional flexural cracks formed outside the constant moment area. These cracks indicated that the concrete cover gripping the splice length began to fail to resist the pull-out forces of the spliced reinforcement. Further loading worsens this horizontal crack, eventu-

ally causing the concrete cover to undergo splitting. The failure of the bond was due to the splitting of the concrete cover that occurred along the splice reinforcement. This failure marks the brittle behaviour of the beam, where the collapse occurred suddenly when the concrete cover in that area was detached.

## 3.2 Load vs deflection

In this study, the relationship between incrementally applied loads on the beam and the resulting deflections was analyzed until the maximum load was reached. Fig. 5 illustrates the process of examining this load-deflection relationship. The results show that deflection increases proportionally with the applied load. The test produces a trilinear load-deflection curve, which demonstrates the effectiveness of the force transfer mechanism during loading. Initially, the curve reflects the elastic behavior of the beam, followed by an increase in stiffness, and finally entering a plastic phase where stiffness significantly decreases (Fig. 6).



**Fig. 5.** Testing process of the splice beam.

For the control beams, the first crack occurred at a load interval between 26.18 and 27.12 kN, marking the end of the first linear phase. After surpassing the first crack load, the curve transitions into a second linear phase until the reinforcement yields. During this phase, the beam maintains relatively high stiffness. Upon reach-

ing the second linear phase limit, a third phase emerges, where small load increments cause significant increases in deflection. This final phase represents the beam's transition to a plastic state, where stiffness drops drastically until failure occurs.

In the beams with splice connections, specimen 0.75-12-NS exhibited a similar trilinear load-deflection behavior, although its stiffness, capacity, and ductility were lower compared to the control beams. The load at the first crack was nearly equivalent to that of the control beams. Beyond this, a second linear phase followed, characterized by sustained stiffness until significant deflection occurred. After this second phase, a third linear phase emerged, where small load increments led to large deflections, indicating the beam had transitioned into a plastic state with drastically reduced stiffness. At this stage, the beam could no longer bear additional loads effectively, leading to failure through a splitting mechanism in the splice connection.

However, specimens 0.75-16-NS and 0.75-19-NS only exhibited two linear phases in their load-deflection curves. These specimens experienced pullout or slippage at the splice reinforcement, causing the lack of a third phase. As shown in Table 6, the reinforcement stress ($f_s$) was less than the yield strength ($f_y$), meaning the reinforcement remained in an elastic state, which explains the absence of the plastic behavior seen in other specimens.

.

### 3.3 Load vs. strain

Strain measurements on reinforcement steel were conducted using a strain gauge specifically for steel connected to a P3 Strain Indicator. This strain gauge was applied to the underside of the longitudinal reinforcement, positioned precisely to cap-
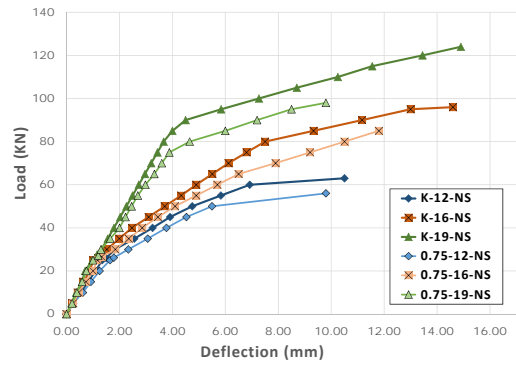


**Fig. 6.** Comparison of load versus deflection.

ture the maximum strain induced by loading. For the control beam, the steel strain gauge was positioned right at the centre of the beam. Meanwhile, for splice beams, the strain gauge was placed at the ends of the splice reinforcement. This placement was explicitly designed to measure the maximum strain occurring as a response to the applied load, providing crucial data for analyzing the structural effectiveness of the beams in handling loads.
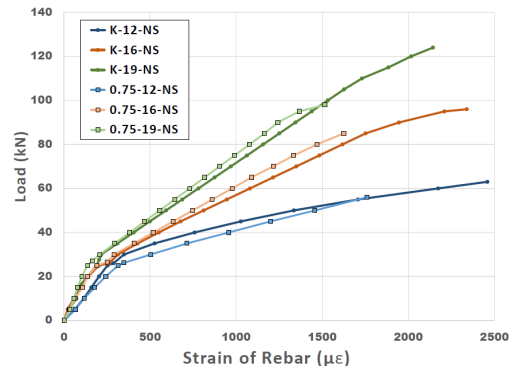


**Fig. 7.** Load vs. Strain in Splice Beam

The smooth strain results shown in Fig. 7 can be explained by the testing method employed and data collection intervals. The beam specimens were loaded using a hydraulic jack with a fixed deflection increment of 5 kN per loading cycle, and the strain data were only recorded at

**Table 6.** Specimen HVFA-SCC properties and test results.

| Beam ID | $d_b$ (mm) | $f_c'$ (MPa) | $0.75l_s$ (mm) | $\rho$ (%) | $P_{cr}$ (kN) | $P_{ult}$ (kN) | $f_s$ (MPa) | $\tau_{test}$ (MPa) | Failure Mode |
|---|---|---|---|---|---|---|---|---|---|
| K-12-NS | 12 | 33 | - | 0.68 | 26.18 | 63 | 492 | - | Flexural |
| K-16-NS | 16 | 33 | - | 1.24 | 26.58 | 96 | 468 | - | Flexural |
| K-19-NS | 19 | 33 | - | 1.76 | 27.12 | 124 | 429 | - | Flexural |
| 0.75-12-NS | 12 | 33 | 300 | 0.68 | 26.15 | 56 | 352 | 3.44 | Splitting |
| 0.75-16-NS | 16 | 33 | 410 | 1.24 | 26.51 | 85 | 325 | 3.11 | Slippage |
| 0.75-19-NS | 19 | 33 | 450 | 1.76 | 27.64 | 98 | 303 | 3.15 | Slippage |

every applied load. As a result, the strain gauges may not have captured every minor crack as it formed, but rather the larger strain changes that occurred at the load intervals. This approach likely smoothed out the strain curve, as smaller crack formations in between the recorded intervals were not detected.

Fig. 7 displays the load versus strain readings for the longitudinal reinforcement of each tested beam. Analysis of the resulting curves reveals distinct trilinear characteristics, with significant changes in slope occurring at the flexural cracking load. Once the flexural cracking load is reached, observations show that the curve becomes flatter, marking the transition to the second phase. The conclusion that can be drawn from this phenomenon is the change in stiffness of the beams as the first flexural cracks occur.

In the control beams, the transition from the second phase linear curve to the third phase occurs after the reinforcement reaches the yield strain. Following the achievement of this yield strain, the curve enters the third linear phase, marked by a drastic increase in strain. This phase continues until the beam ultimately reaches failure. This third phase indicates a high ductility phase, where the beam can still sustain load increases despite significant strain increases, an indication of the beam's ability to absorb energy before finally experiencing structural failure.

For beams with splice length without stirrups, the second linear phase of the load-strain curve ends when the reinforcement reaches a point where strain increases drastically, leading to the failure of the beam. This increase in strain is caused by the expansion of cracks in the concrete, which results in the transfer of load to the steel reinforcement. After reaching this critical point, the load vs. strain curve becomes flatter, indicating a decrease in the beam's stiffness. This change indicates that the beam becomes less capable of sustaining additional loads, and the curve ends at the maximum load point when the beam finally fails. This behaviour highlights the importance of considering the impact of concrete cracking on strain distribution and overall beam stiffness, especially in the design of beams with splice length without stirrups.

### 3.4 Strength index and ductility index

The Strength Index and Ductility Index are vital parameters for evaluating the efficiency of bond strength in splice beams. The Strength Index is defined as the ratio of the maximum load sustained by a splice beam to the maximum load on a control beam. It provides a relative measure of the strength of the splice length in terms of load-carrying capacity. Meanwhile, the Ductility Index is calculated as the comparison between the maximum deflection achieved by the splice beams and the maximum deflection on the control beam, providing insight into the differences in duc-

tility capacity between the two types of beams.

Both indexes play a crucial role in identifying the extent to which splice lengths affect the structural performance of beams, both in terms of strength and ductility. The analysis of the Strength Index indicates the effectiveness of the bond in transferring load. In contrast, the Ductility Index highlights the structure's ability to absorb and distribute energy before reaching failure. The combination of these two indexes provides a comprehensive view of the efficiency of the splice length design in enhancing the overall performance of the beam.

Based on the experimental data obtained, calculations of the Strength and Ductility Indexes are performed. The results of these calculations are presented in Table 7.

Based on the calculations presented in Table 7, it is evident that variations in reinforcement diameter at splice length have a minimal effect on the Ductility Index and Strength Index values. The values of both indexes show insignificant differences between one diameter and another, indicating no significant improvement in the effectiveness of the splice length with respect to increasing reinforcement diameter. These results suggest that, in the context of the experiments conducted, changes in the diameter of splice length reinforcement do not directly contribute to improvements in ductility or overall structural strength of the beams. This indicates that other factors may be more influential in determining the efficiency of bond strength and structural performance of beams with splice length than merely increasing the diameter of the reinforcement.

| Type of Beam | Strength Index | Ductility Index |
|---|---|---|
| 0.75-12-NS | 0.723 | 0.889 |
| 0.75-16-NS | 0.800 | 0.885 |
| 0.75-19-NS | 0.793 | 0.790 |

**Table 7.** Strength Index and Ductility Index of Splice Beams

## 4. Comparison of Bond Strength with Collected Database

The documented splice beam test results available in the literature [34, 36–43] were collected for comparative analysis. The primary objective of this study is to determine whether the test results obtained in our research align with the trends observed in the existing data.

To facilitate an adequate comparison, the normalized bond strength, calculated using the square root of the compressive strength, is plotted against the ratio of splice length to rebar diameter ($l_s/D$). The data collected encompass a compressive strength range of 30 to 104 MPa and a splice length to diameter ratio ($l_s/D$) ranging from 9.52 to 58.1. These data points are illustrated in Fig. 8.

As depicted in Fig. 8, the bond strength of High-Volume Fly Ash Self-Consolidating Concrete (HVFA-SCC) is superior to that of Normal Concrete (NC) and Self-Consolidating Concrete (SCC). The result is evidenced by the HVFA-SCC data points lying above the curves representing NC and SCC. It indicates that HVFA-SCC concrete exhibits enhanced bond strength compared to both NC and SCC concretes.

However, the collected data on HVFA-SCC concrete with plain reinforcement bars is too limited for generating a relationship equation between $l_s/D$ and normalized bond strength. Despite this limitation, the coordinate data points in

Fig. 8 clearly show that the bond strength of HVFA-SCC concrete with plain reinforcement bars is consistently higher than that of NC and SCC (with deformed reinforcement bars). Therefore, it is concluded that HVFA-SCC concrete demonstrates better bond strength compared to both NC and SCC.
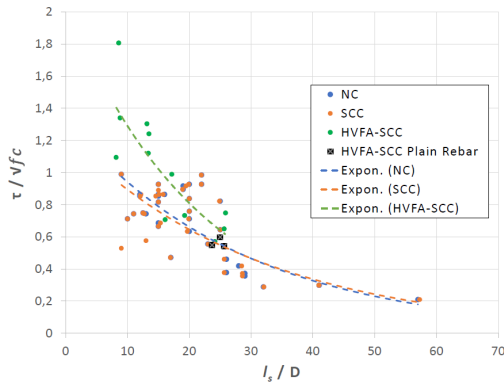


**Fig. 8.** Comparison of bond strength of splice beam specimens with different concrete types.

## 5. Conclusion and Recommendation

Based on the testing data, analysis, and discussions on how reinforcement diameter affects splice beams in HVFA-SCC, the following conclusions are made:

1. **Bond Strength:** The bond strength achieved in HVFA-SCC beams with plain reinforcement bars was measured as 3.44 MPa for bars with a 12 mm diameter, 3.11 MPa for bars with a 16 mm diameter, and 3.15 MPa for bars with a 19 mm diameter.

2. **Crack Patterns:** Control beams exhibited flexural cracks forming at the mid-span, while splice beams exhibited cracks forming at the ends of the splice length in areas of constant moment. As the load increased, these cracks propagated beyond the constant moment areas and into the compression zone, eventually leading to failure.

3. **Failure Modes:** Control beams typically experienced flexural failure, while beams with splice lengths showed splitting failure due to bond failure in the unconfined splice regions.

4. **Splice Length and Reinforcement Diameter:** The reinforcement diameter and splice length did not significantly affect the magnitude of bond strength, though they impacted the required splice length in the tension reinforcement.

### Recommendations:

1. Further research is needed to optimize splice length for improved bond performance, particularly in HVFA-SCC applications with plain reinforcement.

2. Studies should explore how variations in concrete quality, including the use of different fly ash content, affect the performance of HVFA-SCC beams.

3. Future research should include a wider range of variables, such as different types of superplasticizers and varying reinforcement diameters, to fully understand their effects on bond strength.

## Acknowledgment

express our profound gratitude for their invaluable assistance in the completion of this study.

# References

[1] Rohman R, Kristiawan S, Basuki A, Saifullah H. Bond strength between reinforcement and high volume fly ash-self compacting concrete (HVFA-SCC). In: IOP Conference Series: Earth and Environmental Science. vol. 1195. IOP Publishing; 2023. p. 012007.

[2] Jain A, Gupta R, Chaudhary S. Sustainable development of self-compacting concrete by using granite waste and fly ash. Construction and Building Materials. 2020;262:120516.

[3] Nguyen H, Chang T, Shih J. Effects of sulfate rich solid waste activator on engineering properties and durability of modified high volume fly ash cement based SCC. Journal of Building Engineering. 2018;20:123–9.

[4] Stefanec P, Gabrijel I, Kolman D, Pulic S. Impact of fluidized bed fly ash on strength development of self-compacting concrete. In: Creative Construction Conference 2023; 2023. p. 123–9.

[5] Kumar S, Rai B. Synergetic effect of fly ash and silica fume on the performance of high volume fly ash self-compacting concrete. Journal of Structural Integrity and Maintenance. 2022;7(1):61–74.

[6] Singh N, Kumar P, Goyal P. Reviewing the behaviour of high volume fly ash based self compacting concrete. Journal of Building Engineering. 2019;26:100882.

[7] Kumar S, Murthi P, Awoyera P, Gobinath R, Kumar S. Impact resistance and strength development of fly ash based self-compacting concrete. Silicon. 2022;14(2):481–92.

[8] Zulu S, Allopi D. Effects and benefits of using high content of fly ash in concrete. International journal of engineering, sciences and research technology. 2016.

[9] Sabău M, Bompa D, Silva L. Comparative carbon emission assessments of recycled and natural aggregate concrete: Environmental influence of cement content. Geoscience Frontiers. 2021;12(6):101235.

[10] Ngudiyono N. Pemanfaatan Fly Ash sebagai Bahan Subtitusi Parsial Semen pada Beton Memadat Sendiri. Jurnal Teknologi Lingkungan. 2022;23(1):55–61.

[11] Mounika C, Reddy V, Rao M, Shrihari S. Optimization and Development of High-Strength High-Volume Fly Ash Concrete Mixes. International Journal of Recent Technology and Engineering. 2019.

[12] Dar A. Advanced performance of fly ash co-mixtured self-compacting concrete. In: IOP Conference Series: Materials Science and Engineering. vol. 561; 2019. p. 012022.

[13] Grdić Z, Topličić-Ćurčić G, Grdić D, Dodevski ea V. Properties of self-compacting concrete produced with biomass wood ash. Tehnički vjesnik. 2021;28(2):495–502.

[14] Zhao J, Cai G, Yang J. Bond-slip behavior and embedment length of reinforcement in high volume fly ash concrete. Materials and Structures. 2016;49(6):2065–82.

[15] Desnerck P, Lees J, Morley C. Bond behaviour of reinforcing bars in cracked concrete. Construction and Building Materials. 2015;94:126–36.

[16] Dacuan C, Abellana V. Bond Deterioration of Corroded-Damaged Reinforced Concrete Structures Exposed to Severe Aggressive Marine Environment. International Journal of Corrosion. 2021:1–13.

[17] Avadh K, Nagai K. 3D RBSM Analysis of Bond Degradation in Corroded Reinforced Concrete as Observed Using Digital Image Correlation. Materials. 2022;15(18):6470.

[18] Apostolopoulos C, Koulouris K, Apostolopoulos A. Correlation of Surface Cracks of Concrete due to Corrosion and Bond Strength (between Steel Bar and Concrete). Advances in Civil Engineering. 2019;1–12.

[19] Lin H, Zhao Y. Effects of confinements on the bond strength between concrete and corroded steel bars. Construction and Building Materials. 2016;118:127–38.

[20] Moccia F, Fernández Ruiz M, Metelli G, Muttoni A, Plizzari G. Casting position effects on bond performance of reinforcement bars. Structural Concrete. 2021;22(3):1612–32.

[21] Shunmuga Vembu P, Ammasi A. A Comprehensive Review on the Factors Affecting Bond Strength in Concrete. Buildings. 2023;13(3):577.

[22] Mohamed O. Durability and Compressive Strength of High Cement Replacement Ratio Self-Consolidating Concrete. Buildings. 2018.

[23] Ahmad M, Adnan S, Zaidi S, Bhargava P. A novel support vector regression (SVR) model for the prediction of splice strength of the unconfined beam specimens. Construction and Building Materials. 2020;248:118475.

[24] Mousa M. Effect of bond loss of tension reinforcement on the flexural behaviour of reinforced concrete beams. HBRC Journal. 2016;12(3):235–41.

[25] Mousavi S, Dehestani M, Mousavi K. Bond strength and development length of steel bar in unconfined self-consolidating concrete. Engineering Structures. 2017;131:587–98.

[26] Harinkhede S, Supekar G, Ingvale S, Wagaralakar V, Narwade A, Dhomse S. Investigation Of New Techniques In Mechanical Rebar Coupler As An Alternative To Lap Splices. Imperial Journal of Interdisciplinary Research (IJIR). 2016;2(6):1039–41.

[27] Kastiza P, Melidis L, Katakalos K. EXPERIMENTAL & NUMERICAL INVESTIGATION OF LAP-SPLICED R/C COLUMNS UNDER THREE POINT BENDING & AXIAL COMPRESSION. In: 8th International Conference on Computational Methods in Structural Dynamics and Earthquake Engineering; 2021. .

[28] Feldman L, Poudyal U, Cairns J. Proposed development length equation for plain bars. ACI Structural Journal. 2018;115(6):1615–7A.

[29] Robuschi S, Lundgren K, Fernandez I, Flansbjer M. Anchorage of naturally corroded, plain reinforcement bars in flexural members. Materials and Structures. 2020;53(2):1–21.

[30] Rabbat B, Alcocer S, Fiorato A, Jirsa J, Rogowsky D, Anderson ea NS. Building code requirements for structural concrete (ACI 318-08) and commentary. American Concrete Institute; 2011.

[31] S E. Guidelines for self-compacting concrete. Association House; 2002.

[32] Indonesia SN NB. Tata cara pemilihan campuran untuk beton normal, beton berat dan beton massa; 2012.

[33] DP U. Tata cara perencanaan campuran beton berkekuatan tinggi dengan semen portland dan abu terbang. Badan Standar Nasional; 2000.

[34] Rohman R, Kristiawan S, Saifullah H, Basuki A. The development length of tensile reinforcement embedded in high volume fly ash-self compacting concrete (HVFA-SCC). Construction and Building Materials. 2022;348:128680.

[35] Rohman R, Kristiawan S, Basuki A, Saifullah ea HA. Experimental and numerical investigation of the splice length requirement in high volume fly ash-self compacting concrete (HVFA-SCC) beam. International Journal of Applied Science and Engineering. 2021;21(2):1–9.

[36] Türk K, Benli A, Calayir Y. Bond Strength of Tension Lap-Splices in Full Scale Self-Compacting Concrete Beams. Turkish Journal of Engineering & Environmental Sciences. 2008;32(6).

[37] Looney T, Arezoumandi M, Volz J, Myers J. An experimental study on bond strength of reinforcing steel in self-consolidating concrete. International Journal of Concrete Structures and Materials. 2012;6:187–97.

[38] Arezoumandi M, Wolfe M, Volz J. A comparative study of the bond strength of reinforcing steel in high-volume fly ash concrete and conventional concrete. Construction and Building Materials. 2013;40:919–24.

[39] Harajli M, Abouniaj M. Bond performance of GFRP bars in tension: Experimental evaluation and assessment of ACI 440 guidelines. Journal of Composites for Construction. 2010;14(6):659–68.

[40] Karatas M, Turk K, Ulucan Z. Investigation of bond between lap-spliced steel bar and self-compacting concrete: The role of silica fume. Canadian Journal of Civil Engineering. 2010;37(3):420–8.

[41] Huang L, Xu L, Chi Y, Deng F, Zhang A. Bond strength of deformed bar embedded in steel-polypropylene hybrid fiber reinforced concrete. Construction and Building Materials. 2019;218:176–92.

[42] Wu C, Chen M, Chen H. Bond behavior of tension bar at lap splice of SCC beam. Key Engineering Materials. 2018;789:126–30.

[43] Harajli M. Comparison of bond strength of steel bars in normal-and high-strength concrete. Journal of Materials in Civil Engineering. 2004;16(4):365–74.